

# WIRELESS POWER TRANSFER USING BINARY BAT ALGORITHM-BASED BEAMFORMER

TRUYỀN NĂNG LƯỢNG KHÔNG DÂY SỬ DỤNG BỘ ĐỊNH DẠNG BÚP SÓNG DỰA TRÊN THUẬT TOÁN ĐÀN DƠI NHỊ PHẦN

Hoang Van Dao<sup>1</sup>, Nguyen Thi Mai Thuy<sup>1</sup>,  
Nguyen Minh Duc<sup>1</sup>, Nguyen Van Cuong<sup>1</sup>,  
Kieu Xuan Thuc<sup>1</sup>, Hoang Manh Kha<sup>1</sup>, Tong Van Luyen<sup>1,\*</sup>

DOI: <https://doi.org/10.57001/huih5804.2023.069>

## ABSTRACT

Recently, wireless power transfer technology, which is transmitted via radio frequency power, is considered as a promising technology. This technology provides a cost-effective energy supply to low-power devices in the future era of the Internet of Things. However, there will be a large number of devices in electromagnetic environments, so they can interfere with each other. To achieve effective power delivery in space, this paper proposes an efficient beamformer that can focus energy on the direction of the desired people and minimize energy in the direction of undesired people (interferences). This beamformer is based on binary bat algorithm and on the technique of controlling complex weights. The results prove that the proposed beamformer can effectively maintain the main lobe, suppress interferences, and surpass a beamformer based on binary particle swarm optimization in terms of sidelobe suppression ability and computational time.

**Keywords:** *Wireless power transfer, beamforming, binary bat algorithm, interference suppression, antenna array pattern synthesis.*

## TÓM TẮT

Gần đây, công nghệ truyền năng lượng không dây, được truyền qua năng lượng tần số vô tuyến, được coi là một công nghệ đầy hứa hẹn. Công nghệ này cung cấp năng lượng hiệu quả về chi phí cho các thiết bị tiêu thụ điện năng thấp trong kỷ nguyên tương lai của vạn vật kết nối Internet. Tuy nhiên, sẽ có một số lượng lớn các thiết bị trong môi trường điện từ nên chúng có thể gây nhiễu lẫn nhau. Để đạt được hiệu quả phân bố năng lượng trong không gian, bài báo này đề xuất một bộ định dạng búp sóng hiệu quả có thể tập trung năng lượng về hướng của người mong muốn và giảm thiểu năng lượng tại hướng của người không mong muốn (nhiễu). Bộ định dạng búp sóng này dựa trên thuật toán đàn dơi nhị phân và kỹ thuật điều khiển trọng số phức. Kết quả chứng minh rằng bộ định dạng búp sóng đề xuất có thể duy trì hiệu quả búp sóng chính, triệt nhiễu và vượt qua bộ định dạng búp sóng dựa trên thuật toán tối ưu bầy đàn nhị phân về khả năng nén búp sóng phụ và thời gian tính toán.

**Từ khóa:** *Truyền năng lượng không dây, định dạng búp sóng, thuật toán đàn dơi nhị phân, triệt nhiễu, tổng hợp giản đồ bức xạ mảng anten.*

<sup>1</sup>Hanoi University of Industry

\*Email: [luyentv@hau.edu.vn](mailto:luyentv@hau.edu.vn)

Received: 22/10/2022

Revised: 02/02/2023

Accepted: 15/3/2023

## 1. INTRODUCTION

The development and application of physically connected devices have been facing difficult technical challenges. As a new model of power supply, wireless power transfer (WPT) provides a new direction to receive energy for the control of electrical devices, which can reduce excessive dependence on connectivity physics. Focusing on the WPT system, building research, and discussing topics to improve WPT is the future development trend. This novel energy and its transmission mechanism show important implications for the widespread application of renewable energy in daily life [1-4]. Besides, the transmission of electrical energy to devices is a huge loss, not only for the costs and efforts but also for the quality of transmission signals when it comes to large-scale Internet of Things (IoT) connectivity [2, 5]. Interferences in the surroundings of electromagnetic wave transmission are a constant factor in the degradation of transmitted signal quality. To enhance interference suppression and spectrum utilization in radar applications and wireless power transfer, array pattern synthesis has been considered in numerous research papers [6-10]. There are a number of pattern synthesis techniques used to suppress sidelobes, each having advantages and disadvantages, such as weight control, position-only control, and array thinning. Among those, complex weight control in weight control technique has been the best performance for array pattern synthesis or wireless power transfer [10-13].

Recently, metaheuristics such as bat algorithm or binary bat algorithm (BBA) and particle swarm optimization or binary particle swarm optimization (BPSO) have been proven to be efficient global optimization algorithms. These algorithms are used to produce optimal patterns in continuous and discrete optimization problems; they are proven to be superior to traditional optimization techniques as well [14-18]. Beamformers (BF) based on BBA or BPSO can optimize binary numbers and then directly apply them to digital attenuators or digital

phase shifters to control amplitudes and/or phases excited at each element. The aforementioned beamformers are applied for uniform linear arrays, but this kind of array lacks the capacity to scan in space [20-22]. In contrast, the main lobe of the uniform rectangular arrays (URAs) pattern can be controlled in any elevation and azimuth direction in space. Furthermore, URAs are more flexible, producing more symmetrical patterns with deeper sidelobes. WPT and IoT using beamforming technology with interference suppression ability offer several benefits over the wired connection and are applied in numerous applications such as wearable electronics, health care, electric vehicle charging, sensor networks, and consumer electronics [24-26].

This paper proposes a beamformer based on BBA and on the technique of controlling complex weights of URAs of dipole antennas. This beamformer is compared to a beamformer based on binary particle swarm optimization, and the proposed beamformer is proved to be superior to BSPO-based BF in terms of sidelobe suppression ability and computational time. The effectiveness of the proposed beamformer will be evaluated through simulation scenarios.

**2. PROBLEM FORMULATION**

Figure 1 illustrates wireless power transfer technology using beamforming where base stations are equipped with rectangular antenna arrays. In this illustration, antenna arrays are used for location-based services so that base stations with multiple-input-multiple-output can precisely determine where user equipment is located within the network. Besides, base stations equipped with these arrays can enhance the capability of the system to combat fast fading, interference, and noise power thus improving the spectral efficiency and energy efficiency of the system.

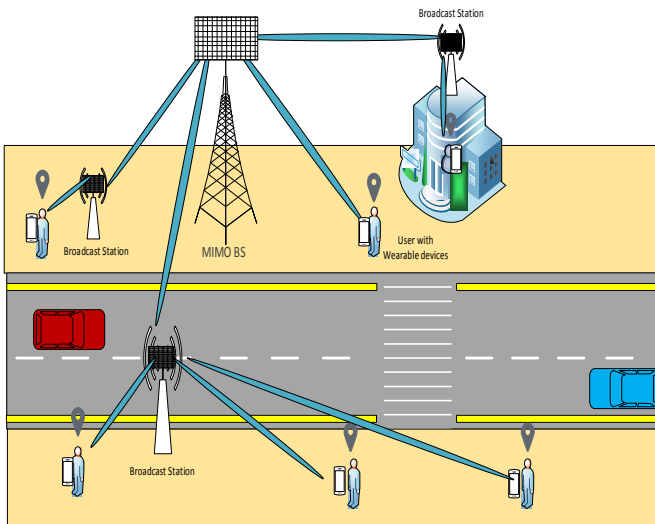


Figure 1. An illustration of wireless power transfer using beamforming

This paper considers a URA with  $M \times N$  halfwave-length antenna (blue dot) as shown in Figure 2. The antenna array pattern can be expressed as [22]:

$$P(\phi, \theta) = EF \cdot AF = EF \sum_{m=0}^{M-1} \sum_{n=0}^{N-1} w_{m,n} e^{j(m\psi_z + n\psi_y)} \quad (1)$$

where: EF and AF are the element factor of the dipole and the array factor of the array at  $(\phi, \theta)$  respectively;  $\psi_z = \kappa d_z \cos(\theta)$ ;  $\psi_y = \kappa d_y \sin(\theta) \sin(\phi)$ ;  $\kappa = \frac{2\pi}{\lambda}$ ;  $w_{m,n} = a_{m,n} e^{j\delta_{m,n}}$  is the complex weight at the  $(m, n)^{th}$  element;  $a_{m,n}$  and  $\delta_{m,n}$  are the amplitude and the phase, respectively.

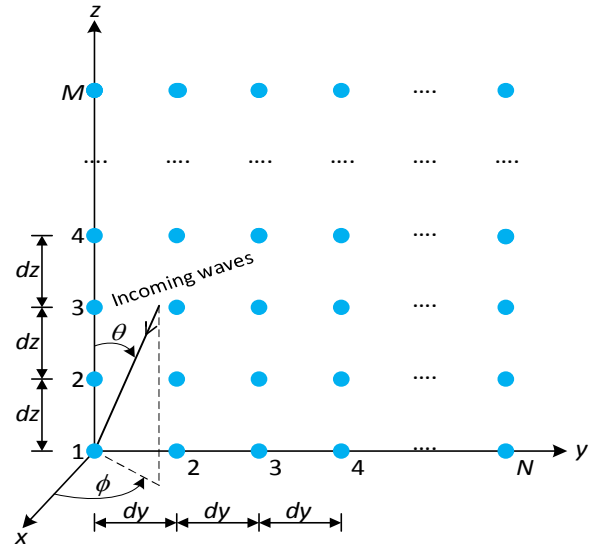


Figure 2. A URA with  $M \times N$  elements

To steer the main lobe toward  $(\phi_0, \theta_0)$ , the phase shift of the  $(m, n)^{th}$  antenna element is equal to [22]:

$$\delta_{m,n} = -\kappa(m d_z \cos(\theta_0) + n d_y \sin(\theta_0) \sin(\phi_0)) \quad (2)$$

The proposed algorithm is used to obtain optimal amplitudes and phases of complex weights that are excited at each element. This algorithm is described in the next section.

**3. THE PROPOSED BEAMFORMER**

The fitness function in this paper is developed for the receiver, but this development is similar for the transmitter. The proposed beamformer is to maintain the main lobe and keep sidelobes at a specified level, while also suppressing interferences. Therefore, the fitness function based on the penalty method [27] can be formulated as follows [19, 20]:

$$F(\delta) = \frac{1}{\xi} \left[ \begin{aligned} & \xi \sum_{i=1}^I [ |P_o(\phi_i, \theta_i)|^2 ] + \\ & \sum_{\substack{\theta = 180^\circ \\ \phi = \phi_0, \theta = 0^\circ \\ \phi = 90^\circ}} [ |P_o(\phi, \theta) - P_r(\phi, \theta)|^2 ] + \\ & \sum_{\theta = \theta_0, \phi = -90^\circ} [ |P_o(\phi, \theta) - P_r(\phi, \theta)|^2 ] \end{aligned} \right] \quad (3)$$

where:  $\xi$  is the penalty parameter that is chosen based on the first simulation scenario in the next section;  $I$  is the total number of interfering signals;  $(\phi_i, \theta_i)$  is the direction of the  $i^{\text{th}}$  interfering signal;

$$\xi \sum_{i=1}^I [|P_o(\phi_i, \theta_i)|^2] \tag{4}$$

is used to place  $I$  nulls at  $(\phi_i, \theta_i)$ .

$$\sum_{\phi=\phi_0, \theta=0^\circ}^{\theta=180^\circ} [|P_o(\phi, \theta) - P_r(\phi, \theta)|^2] + \sum_{\theta=\theta_0, \phi=-90^\circ}^{\phi=90^\circ} [|P_o(\phi, \theta) - P_r(\phi, \theta)|^2] \tag{5}$$

for  $(\phi, \theta) \neq (\phi_i, \theta_i)$  are used to maintain the optimized pattern  $P_o(\phi, \theta)$  with as little interference as possible to the reference pattern  $P_r(\phi, \theta)$ ;  $P_o(\phi, \theta)$  and  $P_o(\phi_i, \theta_i)$  are patterns optimized by BPSO or BBA at  $(\phi, \theta)$  and  $(\phi_i, \theta_i)$ , respectively.

The proposed algorithm, which is displayed in Figure 3, is used to obtain the optimal weights (both amplitude and phases). This algorithm is described as follows: (i) Setting the parameters of the BBA and the antenna array (a block with a red border); (ii) then implementing the BBA search mechanism (green-bordered blocks) (see more details in [14]); (iii) after finding optimal weights and the value of the fitness function. Finally, optimal weights are obtained to produce nulled patterns (a block with a blue border).

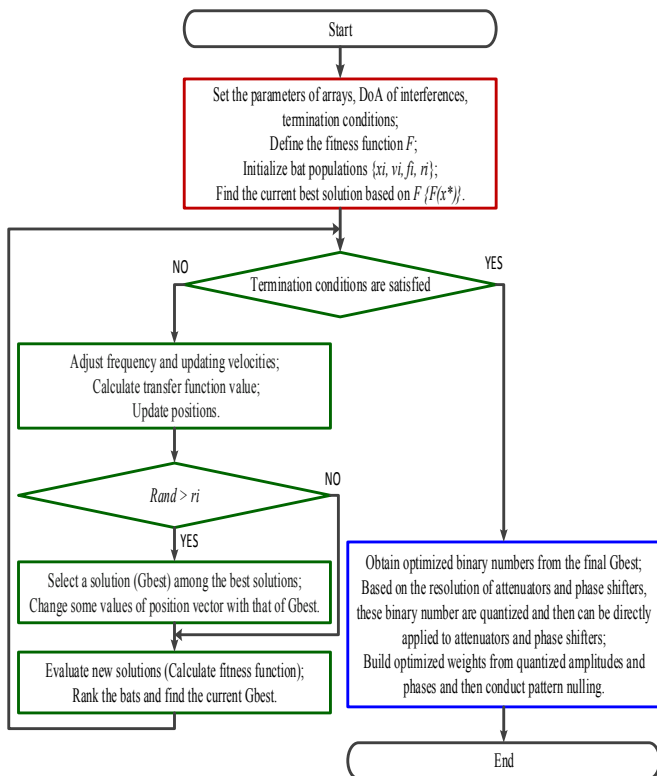


Figure 3. The flowchart of the proposed algorithm

#### 4. NUMERICAL RESULTS

The performance of the proposed beamformer for interference suppression is evaluated via four scenarios in this section. CST Studio Suite 2019 is used to design dipole antennas (shown in Figure 4) for the URA with a resonant frequency of 2.4GHz. All simulation scenarios use the following common parameters: the element factor is the dipole antenna pattern shown in Figure 4, 6-bit digital attenuator and phase shifters with  $M = N = 7$  and  $d_y = d_z = 70$  millimeters, the reference pattern  $P_r(\phi, \theta)$  is selected as the Chebyshev pattern with sidelobe level (SLL) of  $-25\text{dB}$ , the population is  $\text{pop} = 50$ , and the iteration is  $\text{iter} = 1$  from the third scenario onwards. BBA and BPSO solutions are randomly initialized except for one solution that is initialized with weights of the reference pattern. Due to the randomness of the initial solutions, the performance of two BFs based on BBA and BPSO will be verified by averaging the results of 1000 independent simulations for each scenario.

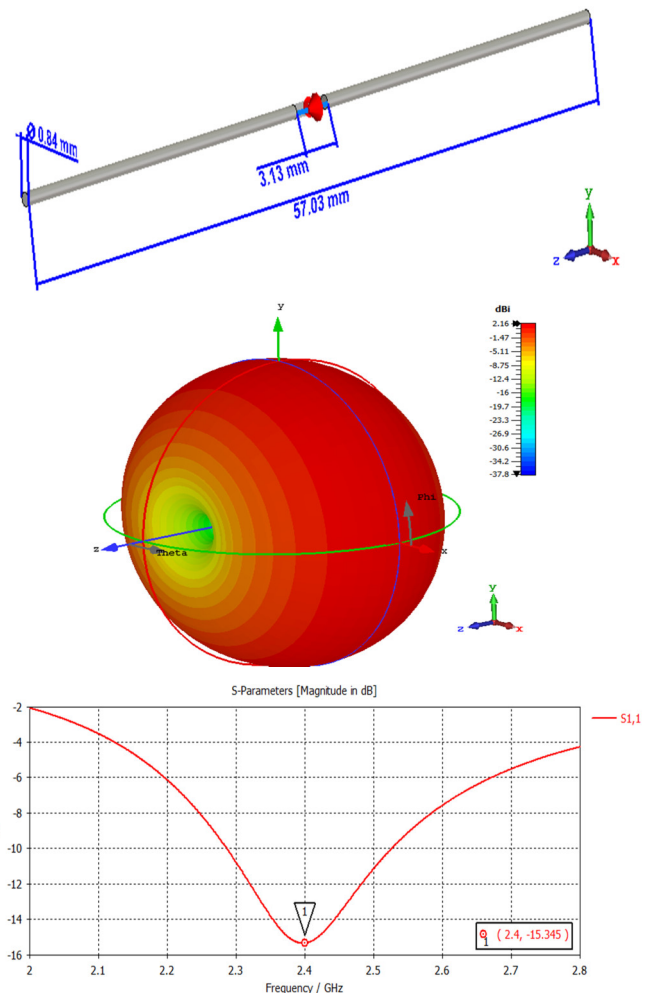


Figure 4. The characteristics of a dipole antenna designed in CST

##### 4.1. Penalty Parameter $\xi$

In the fitness function, the penalty parameter is an undefined parameter that is determined in the first scenario. To point out the right value of this parameter, the

max sidelobe level (max SLL) and the null depth level (NDL) at  $(\phi_i, \theta_i) = (40^\circ, 90^\circ)$  are evaluated with penalty parameter values from  $10^0$  to  $10^5$  with pop = 50 and iter = 200. The results, which are shown in Figure 5 and Figure 6, indicate that the deeper the null and the max SLL of optimized patterns likewise change significantly when are large enough. The value chosen for the next scenarios should be 2500 to balance the trade-off between NDL and max SLL.

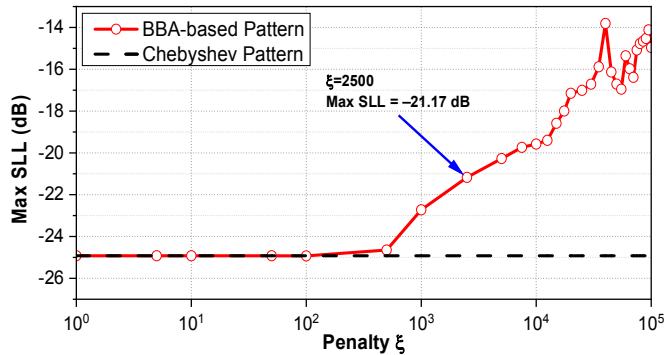


Figure 5. The max SLL of optimized pattern with different penalty values

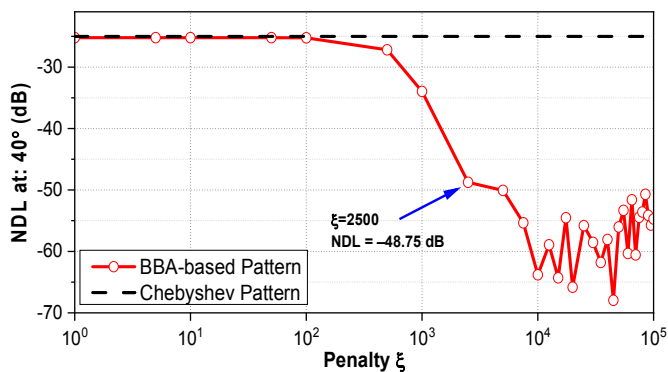


Figure 6. The NDL of optimized pattern with different penalty values

### 4.2. Characteristics of Convergence

This scenario compares the fitness function's value when a single null is placed at the peak of the Chebyshev pattern  $(\phi_i, \theta_i) = (40^\circ, 90^\circ)$ . BBA-based BF (the proposed beamformer) is investigated with various population sizes over 200 iterations. Based on the results shown in Figure 7, this beamformer has taken 7, 2, 1, and 1 iterations to approximately achieve  $F \leq 1$  corresponding to pop = 10, 30, 50 and 70, respectively. For purposes of illustration, pop = 50 and iter = 1 are chosen for the next scenarios.

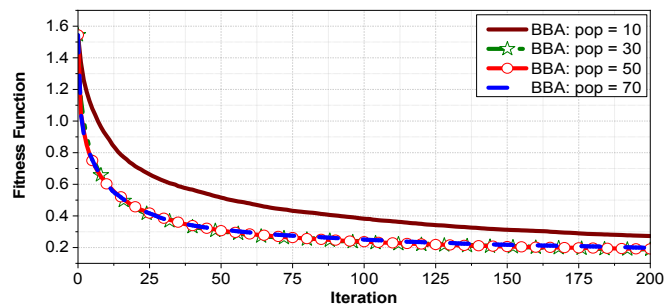


Figure 7. The fitness function of BBA-based BF with different population sizes

In Figure 8, the fitness function of BBA-based BF is compared to that of BPSO-based BF with pop = 50 and iter = 200. Overall, the one based on BBA converges much more quickly than that based on BPSO. To reach  $F \leq 0.6$ , moreover, BPSO-based BF requires 5249.40 milliseconds, which is 13 times longer than that of the proposed beamformer that only takes 410.62 milliseconds.

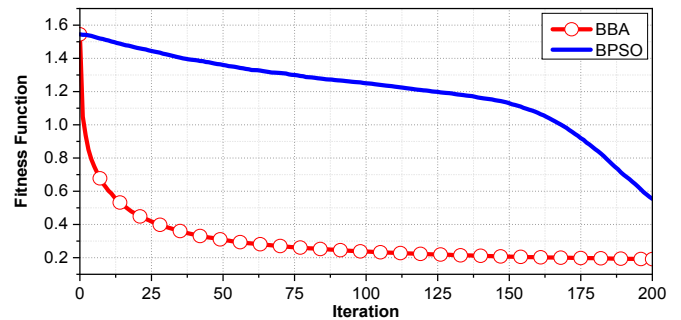


Figure 8. The fitness function of BFs based on BBA and BPSO.

### 4.3. Effective Null-Steering Capability

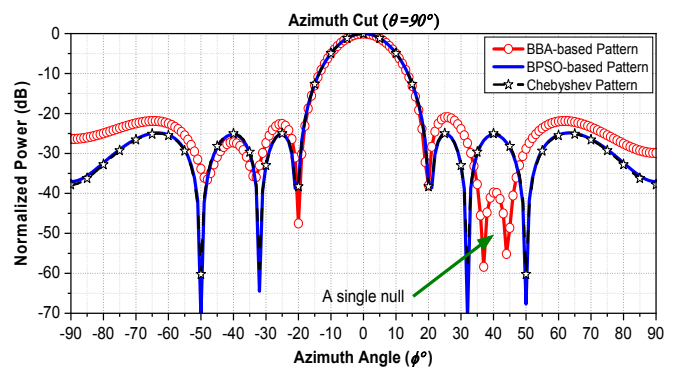


Figure 9. The 2D optimized patterns with a single null

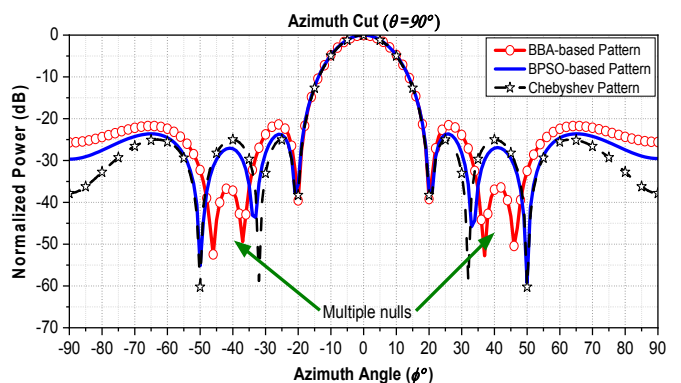


Figure 10. The 2D optimized patterns with multiple nulls

The scenario illustrated in Figure 9, and Figure 10, compare the BBA and BPSO-optimized pattern with one null and multiple nulls, respectively. The results indicate that BBA-based BF is superior to BPSO-based BF in terms of suppressing sidelobes as well as imposing nulls. For example, the proposed beamformer suppresses the peak of a sidelobe at  $(\phi_i = 40^\circ, \theta_i = 90^\circ)$  down to  $-39.78\text{dB}$  while BPSO-based BF does not seem to be able to suppress this sidelobe. One more proof of interference suppression

ability, the BBA-based BF imposes two multiple nulls at ( $\phi_i = -40^\circ$  and  $40^\circ, \theta_i = 90^\circ$ ) that are less than  $-35\text{dB}$ , while BPSO-based one suppresses sidelobes in either direction of interfering signals to be negligible.

**4.4. Optimized Patterns with Different Resolutions**

In addition to being constrained to a fixed direction as in the aforementioned scenarios, the main lobe of the proposed beamformer can also be steered. In the final scenario, the proposed beamformer is evaluated by steering the main lobe toward ( $\phi_0 = 10^\circ, \theta_0 = 80^\circ$ ) and placing nulls in the range of ( $\phi_i = [-35^\circ: -25^\circ], \theta_i = 80^\circ$ ). Based on the results of 2D patterns in Figure 11, despite using 4-bit devices (including attenuators and phase shifters), sidelobes in direction of interferences of the ideal pattern and that of the pattern simulated in CST are both suppressed. Despite the impacts of mutual coupling simulated by CST, BBA-based BF can still maintain the main lobe and suppress the sidelobes in the region of interfering signals. Besides, the proposal’s efficiency is also evaluated when using different resolutions of attenuators and phase shifters under the same conditions as above. The results for evaluation are simulated in CST and shown in Figure 12. In all three cases, the main lobe is maintained and sidelobes in the interference region are suppressed; however, as the number of bits for attenuators and phase shifters decreases, the number of sidelobes increases, and the higher sidelobes appears. To balance the trade-off between the cost and performance, therefore, digital attenuators and phase shifters with 4 bits or greater should be used.

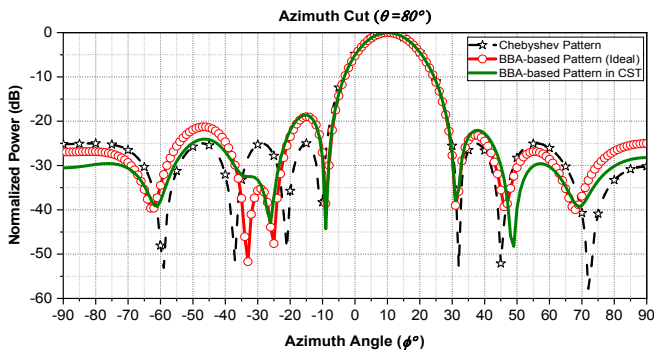
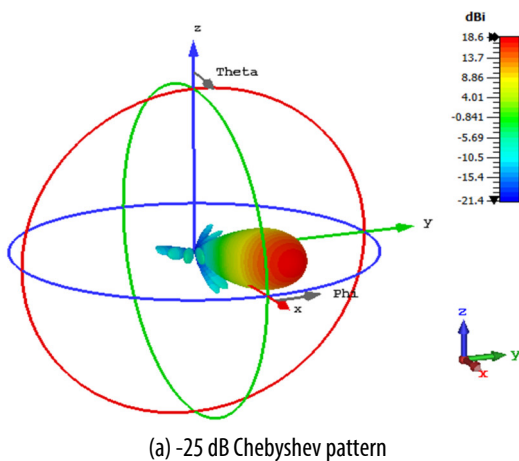
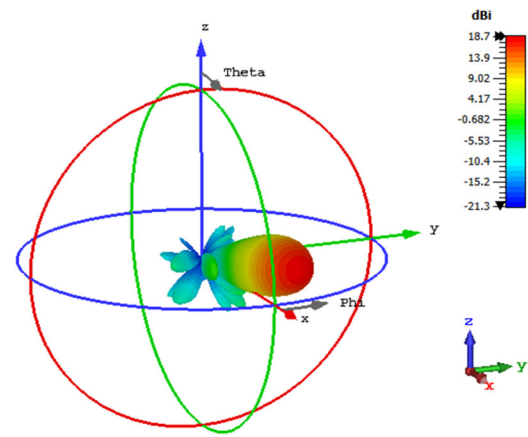


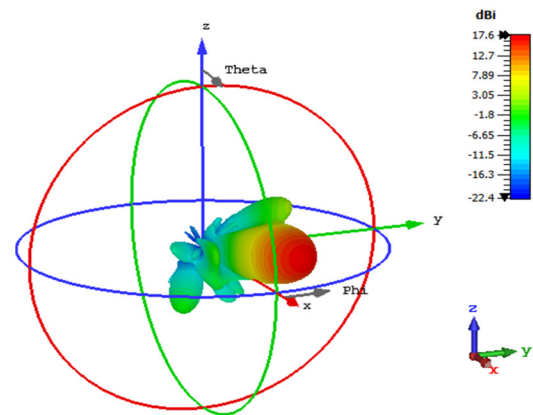
Figure 11. The 2D patterns when using 4-bit devices



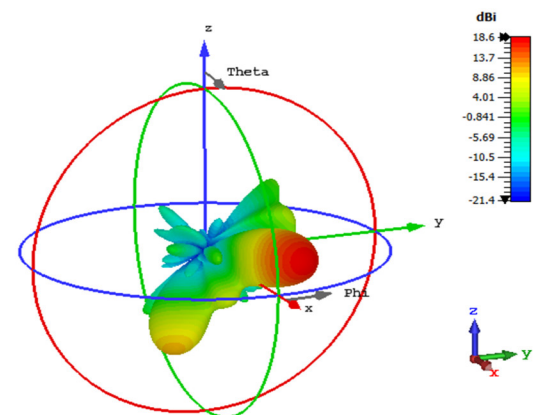
(a) -25 dB Chebyshev pattern



(b) 4-bit devices



(c) 3-bit devices



(d) 2-bit devices

Figure 12. The 3D patterns with the different resolutions of devices.

**5. CONCLUSION**

This paper proposed a beamformer based on BBA for URAs of dipole antennas. Various simulation scenarios were conducted to verify the ability to set nulls in sidelobe regions and the effect of the resolution of digital attenuators and phase shifters on optimal patterns. Additionally, the proposal is proved to be superior to BPSO-based BF in terms of maintaining the main lobe and imposing nulls. Besides, the paper suggested that BBA-based BF should use 4-bit phase shifters to balance the trade-off between cost and performance. In the future,



unknown interferences, interferences entering the main lobe, mutual coupling compensation, or approaches for reducing the hardware requirements should be considered.

#### ACKNOWLEDGEMENT

This research is supported by Hanoi University of Industry (HaUI) [grant number 18-2022-RD/HĐ-ĐHCN].

#### REFERENCES

- [1]. M. Song, et al., 2021. *Wireless power transfer based on novel physical concepts*. Nature Electronics, vol. 4, no. 10, pp. 707–716.
- [2]. H. Zhang, et al., 2022. *Near-field wireless power transfer for 6G Internet of Everything mobile networks: Opportunities and challenges*. IEEE Communications Magazine, vol. 60, no. 3, pp. 12–18.
- [3]. Z. Zhang, H. Pang, A. Georgiadis, C. Cecati, 2019. *Wireless power transfer—An overview*. IEEE Transactions on Industrial Electronics, vol. 66, no. 2, pp. 1044–1058.
- [4]. A. Mahesh, B. Chokkalingam, L. Mihet-Popa, 2021. *Inductive wireless power transfer charging for electric vehicles - A review*. IEEE Access, vol. 9, pp. 137667–137713.
- [5]. P. S. Yedavalli, T. Riihonen, X. Wang, J. M. Rabaey, 2017. *Far-field RF wireless power transfer with blind adaptive beamforming for Internet of Things devices*. IEEE Access, vol. 5, pp. 1743–1752.
- [6]. G. Charis, N. Showme, 2017. *Beamforming in wireless communication standards: A survey*. Indian Journal of Science and Technology, vol. 10, no. 5, pp. 1–5.
- [7]. R. Haupt, 2010. *Antenna arrays: A computational approach*. Hoboken, NJ, USA: Wiley, pp. 156–176; 484–515.
- [8]. T. V. Luyen, T. V. B. Giang, 2017. *Interference suppression of ULA antennas by phase-only control using bat algorithm*. IEEE Antennas and Wireless Propagation Letters, vol. 16, pp. 3038–3042.
- [9]. T. V. Luyen, T. V. B. Giang, 2018. *Null-steering beamformer using bat algorithm*. Applied Computational Electromagnetics Society Journal, vol. 33, no. 1, pp. 23–29.
- [10]. T. V. Luyen, T. V. B. Giang, 2018. *Bat algorithm based beamformer for interference suppression by controlling the complex weight*. REV Journal on Electronics and Communications, vol. 7, no. 3-4.
- [11]. T. V. Luyen, H. M. Kha, N. V. Cuong, 2022. *Array pattern synthesis: An approach inspired from convex optimization*. Journal of Science and Technology, Hanoi University of Industry, vol. 58, pp. 166–169.
- [12]. T. V. Luyen, N. V. Cuong, L. Duy, 2022. *An effective beamformer for interference mitigation*. Intelligent Systems and Networks, Springer Nature Singapore, vol. 471, pp. 630–639.
- [13]. T. V. Luyen, N. V. Cuong, 2023. *An effective beamformer for interference suppression without knowing the direction*. International Journal of Electrical and Computer Engineering, vol. 13, no. 1.
- [14]. S. Mirjalili, S. M. Mirjalili, X.S. Yang, 2013. *Binary bat algorithm*. Neural Computing and Applications, vol. 25, no. 3-4. Springer Science and Business Media LLC, pp. 663-681.
- [15]. S. Mirjalili, A. Lewis, 2013. *S-shaped versus V-shaped transfer functions for binary particle swarm optimization*. Swarm and Evolutionary Computation, vol. 9, pp. 1–14.
- [16]. T. V. Luyen, N. V. Cuong, 2021. *An adaptive beamformer utilizing binary bat algorithm for antenna array pattern nulling*. Journal of Science and Technology, Hanoi University of Industry, vol. 57, pp. 52–57.
- [17]. T. V. Luyen, H. M. Kha, N. V. Tuyen, T. V. B. Giang, 2021. *An efficient ULA pattern nulling approach in the presence of unknown interference*. Journal of Electromagnetic Waves and Applications, vol. 35, no. 1, pp. 1–18.
- [18]. T. V. Luyen, et al., 2022. *Null-steering beamformers for suppressing unknown direction interferences in sidelobes*. Journal of Communications, vol. 17, no. 8, pp. 600-607.
- [19]. H. M. Kha, T. V. Luyen, N. V. Cuong, 2022. *A null synthesis technique-based beamformer for uniform rectangular arrays*. in 2022 International Conference on Advanced Technologies for Communications (ATC 2022), presented on 20th October 2022 at Fortuna Hotel Hanoi (Accepted).
- [20]. H. M. Kha, T. V. Luyen, N. V. Cuong, 2022. *An efficient beamformer using phase-only control for interference suppression*. Journal of Communications, 2022 (Accepted).
- [21]. T. V. Luyen, N. V. Cuong, 2022. *An efficient beamformer for uniform rectangular arrays*. Journal of Science & Technology, Hanoi University of Industry Vol. 58 - No. 6A.
- [22]. C. A. Balanis, 2016. *Antenna theory: Analysis and design*, 4th ed. John Wiley and Sons, pp. 348–360.
- [23]. S. Shen, B. Clerckx, 2021. *Joint Waveform and Beamforming Optimization for MIMO Wireless Power Transfer*. IEEE Transactions on Communications, vol. 69, no. 8, pp. 5441–5455.
- [24]. G. Monti, et al., 2017. *Wireless power transfer with three-ports networks: Optimal analytical solutions*. IEEE Transactions on Circuits and Systems I: Regular Papers, vol. 64, no. 2, pp. 494–503.
- [25]. Feng, B. Clerckx, Y. Zhao, 2022. *Waveform and beamforming design for intelligent reflecting surface aided wireless power transfer: single-user and multi-user solutions*. IEEE Transactions on Wireless Communications, vol. 21, no. 7, pp. 5346–5361.
- [26]. S. Shen, B. Clerckx, 2021. *Beamforming optimization for MIMO wireless power transfer with nonlinear energy harvesting: RF combining versus DC combining*. IEEE Transactions on Wireless Communications, vol. 20, no. 1, pp. 199–213.
- [27]. Ö. Yeniay, 2005. *Penalty function methods for constrained optimization with genetic algorithms*. Mathematical and computational Applications, vol. 10, no. 1, pp. 45–56.

#### THÔNG TIN TÁC GIẢ

**Hoàng Văn Đạo, Nguyễn Thị Mai Thủy, Nguyễn Minh Đức, Nguyễn Văn Cường, Kiều Xuân Thực, Hoàng Mạnh Kha, Tống Văn Luyên**  
 Trường Đại học Công nghiệp Hà Nội